GeoConvention 2015
GEOSCIENCE
new horizons
Telus Convention Centre • 4-8 May 2015 • Calgary, AB Canada

From the lab to real scale: simulation of seismic surveillance in viscoelastic media under varying physical conditions.

Anton Biryukov, Nicola Tisato, Giovanni Grasselli
Department of Civil Engineering, University of Toronto

Summary

Estimation of attenuation of the seismic waves in viscoelastic media is important for the quality of geophysical methods relying on processing the recorded waveforms (Madonna and Tisato [2013], Marelli et al. [2010], Tisato and Quintal [2014]). The purpose of this particular contribution is twofold:(i) propose a methodology to numerically estimate attenuation in the material of interest based on laboratory data; (ii) demonstrate that attenuation can vary with the physical conditions of the medium and how that variation affects signal propagation on the real scale.

Introduction

There is increasing interest in monitoring changes in the subsurface over time by means of repetitive (i.e. time-lapse) measurements. Reservoir seismology researchers have spent decades in developing 3D and 4D time-lapse imaging and inversion techniques using active sources and large sensor arrays. The extraction of hydrocarbons or injection of water can cause deformation and induce microearthquakes which may interfere with the production process and cause societal concern. Monitoring these effects is increasingly important for optimal production and reservoir management.

Time-lapse imaging involves comparing snap-shot images taken over time, e.g. a section of the reservoir before and after gas injection. Waveform analysis may be applied to locate the areas of anomalous pressure or water saturation (Manukyan et al. [2012]). For example, research projects worldwide investigates the application of non-intrusive seismic monitoring techniques of potential high-level radioactive waste (HLRW) repositories. HLRW are generally enveloped in bentonite barriers. The temperature (T), pressure, and water content (W_c) of bentonite is expected to increase dramatically over a few years after completion due to radioactive decay of HLRW, swelling of the clay and water saturation. As a results, the physical state is altered, which may jeopardize the integrity of the barrier (Tisato and Marelli [2013]).Seismic monitoring may serve as a non-intrusive tool to track the condition of the barrier.Regardless of application, a common requirement has to be satisfied: the difference in the recorded signals must be well discernible and reflect only the changes in the medium properties (Marelli et al. [2010]). Therefore, numerical investigation of the procedure in the geometry of interest should be conducted and thoroughly analyzed to aid in design and optimization of the monitoring system.

Signal characteristics depend on the media they travel through. One of the major factors, affecting the amplitudes, is called attenuation. It depends on the physical properties of rock and its fluid content. Higher values of attenuation coefficient ($\frac{1}{Q}$) correspond to greater reduction in seismic amplitude. As high attenution greatly affect the signals' amplitudes and relative phases, it has to be taken into account for better analysis that employs numerical modelling. In this contribution, we numerically estimate the effective attenuation in bentonite as a function of T and W_c and show an example of how the variation of W_c and T affects the signal propagating through the repository.

Theory and Methods

Numerical setup

Tisato and Marelli [2013] measured the longitudinal and transverse ultrasonic wave propagation velocities in bentonite as a function of T and W_c, reproducing the conditions expected at a HLRW waste repository. Following the iterative procedure described in Biryukov et al. [2014] we simulated the propagation of ultrasonic waves in a 2D

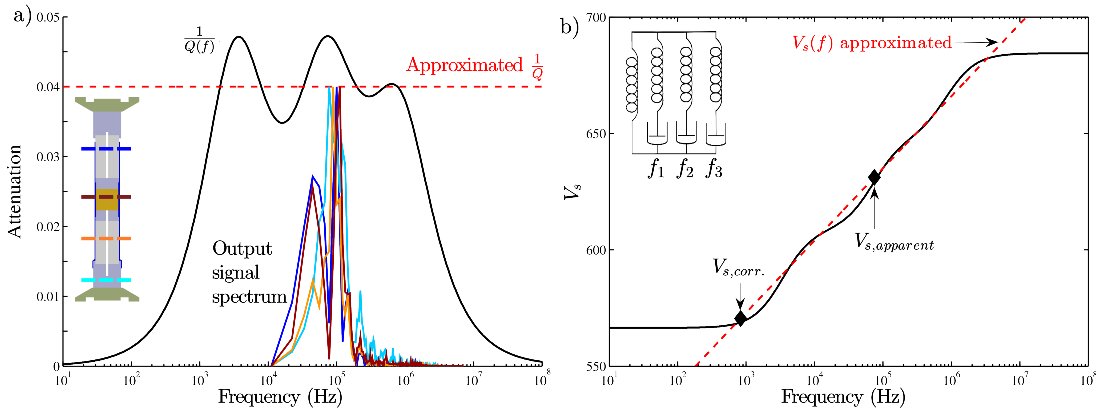

Figure 2. (a) $\frac{1}{Q(f)}$ as a function of frequency approximates constant $Q = 25$ in 1 kHz – 1 MHz bandwidth. Note that the signal spectrum remains within the set frequency range at any cross section of the setup (only 4 are shown for clarity). (b) The mechanical representation of linear viscoelastic model (inlet) and corresponding dispersion of S-wave velocity.

numerical model representing the ultrasonic facility accomodating a bentonite sample (Figure 1). The viscoelastic parameters utilized for the materials are reported in Figure 1 (Auerkari [1996], Boyer and Gall [1984], Lakes [2009]).

Running simulations with fixed T and W_c and varying attenuation for P- and S-waves in bentonite, we compare the numerical and experimental signals in search of the maximum overlap. The value of attenuation, corresponding to the best overlapping simulation, is then regarded as attenution, specific to the fixed values of T and W_c.

Attenuation modelling

Here we define attenuation by the convention proposed by O'Connell and Budiansky [1978]: $\frac{1}{Q} = \frac{M_i}{M_r}$, where M_r and M_i are the real and imaginary parts of the complex modulus respectively.

We used a "generalized standard linear solid" (GSLS) model (Liu et al. [1976]) to create the linear viscoelastic rheological model of bentonite samples. The model (Figure 2,b) is described by an optimization variable τ (Blanch et al. [1995]) and a set of relaxation frequencies f_1, f_2, f_3, representing each Maxwell body. The numerical solver attempts to find optimum parameters of the elements within a set frequency range. Optimum parameters minimize numerically the integrated deviation of the $\frac{1}{Q(f)}$ from the desired attenuation value thus providing the best approximation of a given constant $\frac{1}{Q}$-spectrum :

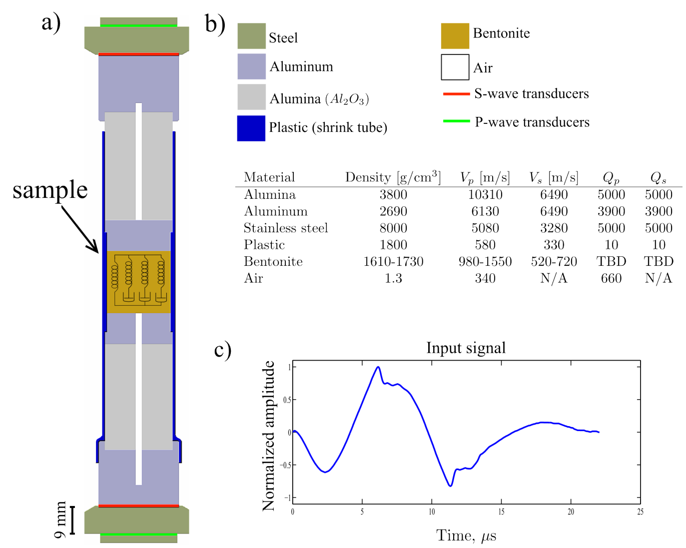

Material	Density [g/cm^3]	V_p [m/s]	V_s [m/s]	Q_p	Q_s
Alumina	3800	10310	6490	5000	5000
Aluminum	2690	6130	6490	3900	3900
Stainless steel	8000	5080	3280	5000	5000
Plastic	1800	580	330	10	10
Bentonite	1610-1730	980-1550	520-720	TBD	TBD
Air	1.3	340	N/A	660	N/A

Figure 1. (a) Schematic diagram of the ultrasonic apparatus employed in the experiments to measure V_p and V_s and used for iterative attenuation estimation (b) Material parameters used in the numerical simulations.The elastic moduli and density of bentonite vary with the temperature and its water content Tisato and Marelli [2013]; therefore we provide the range of values for V_p, V_s, and ρ that were assigned during attenuation estimation. (c) Normalized input signal sent to the emitter

$$\int_{f_1}^{f_2} [\frac{1}{Q(f, f_1, f_2, f_3, \tau)} - \frac{1}{Q'}]^2 df \longrightarrow \min \quad (1)$$

This optimization is performed for the desired $\frac{1}{Q}$ for both P- and S-waves. The resultant attenuation curve has a characteristic shape of multiple peaks in series, located at different relaxation frequencies (2). In the experimental framework, Tisato and Marelli [2013] measured apparent S-wave velocities in bentonite samples at 100 kHz ($V_{s,apparent}$ in Figure 2,b). In order to numerically propagate the signal at the correct velocity (i.e. measured apparent velocity), the input value for bentonite V_s was corrected according to the dispersion curve and the dominant frequency of the signal. The $V_s(f)$ curve was interpolated within the attenuation frequency range with the input value corresponding to the lowest frequency in the range. The same procedure is then applied to the

P-wave velocity model.

Examples and Results

In this section we report the results: the estimation of attenuation in bentonite as a function of temperature and water content, and typical synthetic seismograms obtained simulating the propagation of elastic waves in an HLRW in which T and W_c of bentonite vary.

Attenuation estimation

We employed the ultrasonic shear wave propagation data recorded for four bentonite samples (10%, 20%, 35% and 52% water-content) that were progressively heated in four steps of 10° C from 30° C to 70° C. Therefore, the values of attenuation for P- and S-waves were estimated on a 4×5 grid in the $W_c - T$ domain. For the first set of iterations the procedure revealed the location of the series of minima at $Q_p \in (9, 30)$ and $Q_s \in (4, 15)$. The second iteration refined the region by further discretization into 10×10 grid points. The procedure was then repeated for every node on $T - W_c$-grid. The resultant surface plots of quality factors are illustrated in Figure 3. Our results clearly demonstrate that attenuation in bentonite at fixed temperature T is strongly affected by the water content, with a presence of a distinct minimum at $W_c = 20\%$. However, both quality factors tend to follow similar trend and show no significant variation with respect to temperature T at fixed values of W_c.

Modified GTS framework simulations

As we evaluated the attenuation properties of bentonite under variable physical conditions, we modelled active seismic monitoring procedure in the modified framework of the GTS experiment. To represent the evolution of bentonite's physical conditions, we chose six cases - combinations of T and W_c (Figure 3). The setup follows the description of the site monitoring system described in Marelli et al. [2010]. The seismic energy was released in a form of 3 kHz center frequency Ricker P-wave explosion and recorded by the acquisition system (Figure 4). The geometry of cross section of the tunnel (Figure 4), the relative source and receivers positions, and the results of corresponding numerical simulations are provided in Figure 4, respectively.

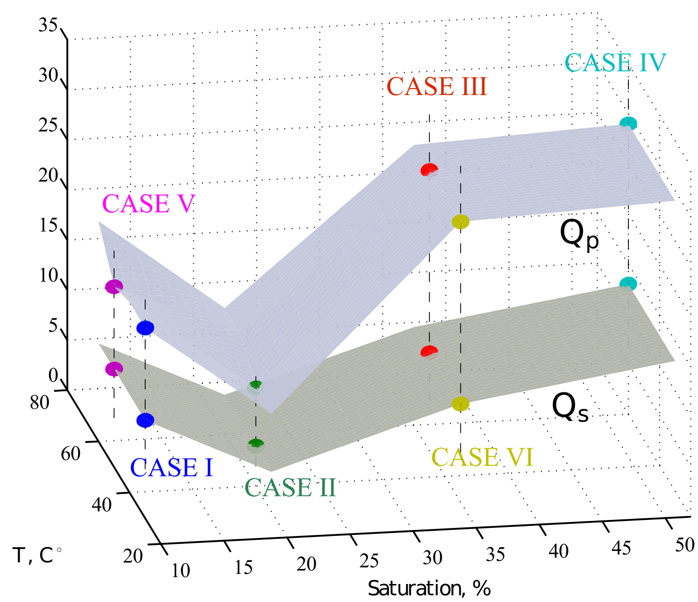

Figure 3. Distribution of Q_p and Q_s in bentonite as a function of temperature and water content: interpolated $Q_p(T, W_c)$ and $Q_s(T, W_c)$ surface plots

Conclusions

Similarity in Q_p and Q_s behavior (i.e. the overall trend and minimum location) suggests that attenuation mechanisms responsible for P- and S-wave dissipation are likely to be similar and exhibit minor variation due to T in the range of 30°-70° C. The magnitude of the variation might also indicate that bentonite's intrinsic structure does not experience significant changes due to temperature increase in the said range compared to the changes caused by water content increase. Consequently one may observe minimal discrepancies in the first arrivals between seismograms, recorded at fixed W_c with variable T (compare Case III versus Case VI, or Case I versus Case V), than recorded at fixed T with variable W_c (compare Case I and Case VI). The coda of the signal, however, shows satisfactory variation among the modelled cases.

The first arrivals recorded by receiver #9 and #10 (Figure 4) are ~ 10 times lower than those recorded by receivers #3 and #4. However, a relatively strong event is observed shortly after, located around $3 - 4.5$ ms. This arrival corresponds to a wave train passing through the interior of the tunnel and is therefore delayed and attenuated. The proximity of the receiver to the line passing through the source and the center of symmetry results into a higher recorded amplitude and subsequently higher signal-to-noise ratio (compare receivers #9 and #10, Figure 4). Since the difference in traces at the time interval is reflected both by the decay amplitude and the phase shift between peaks, we suggest favoring this informative part of the signal over the first arrivals during the analysis employing the in-barrier receivers.

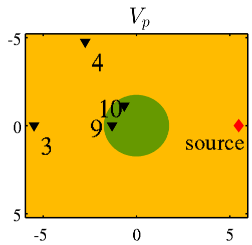

	Case I	Case II	Case III	Case IV	Case V	Case VI
T	30	40	50	60	50	30
W_c	10	20	35	52	10	35
V_p [m/s]	1100	1193	1278	1494	1054	1309
V_s [m/s]	567	617	665	703	547.5	680
Q_p	19	10	28	30	18	28
Q_s	10	4	10	13	10	10
ρ [g/cm^3]	1620	1610	1730	1630	1620	1730

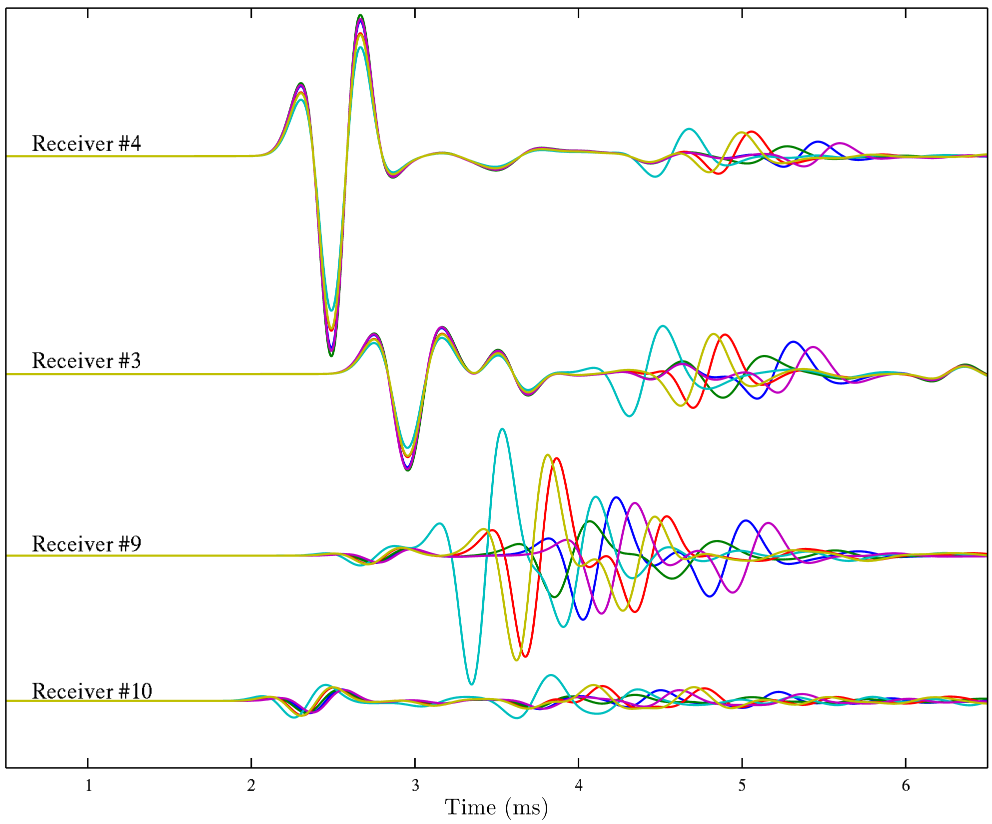

Figure 4. (a) Schematic diagram of the tonnel cross section B and monitoring system, the viscoelastic parameters of the materials employed (Table) and (b) seismograms, corresponding to modelled bentonite physical conditions (cases).The receivers are indicated as black triangles, the source location is shown in red diamond. The table summarizes the viscoelastic parameters that were assigned to bentonite on a case-by-case basis. Seismic traces are colored based on the physical conditions (modeling case) they refer to.

The distance between the source and the receiver is an important factor that affects the quality of the postclosure surveillance (Manukyan et al. [2012], Marelli et al. [2010]). The higher the fraction of the bentonite component in the total travel path, the more pronounced become the differences in the recorded signals. One of the ways to achieve a maximum fraction of the bentonite component in the total travel path of the signal is to place the seismic source inside the tunnel. This will force the seismic energy to travel substantial distance in the tunnel. As a result, the first arrivals registered in the host rock, will be affected by bentonite attenuation, facilitating the waveform comparison.

Acknowledgments

The authors would like to express gratitude to Simon Harvey of the University of Toronto's Civil Engineering Departments for his suggestions and revisions.

References

Pertti Auerkari. *Mechanical and Physical Properties of Engineering Alumina Ceramics*. Technical Research Centre of Finland, 1996. ISBN 9789513849870.

A. Biryukov, N. Tisato, and G. Grasselli. Workflow to numerically reproduce laboratory ultrasonic datasets. oct 2014.

Joakim O. Blanch, Johan O. A. Robertsson, and William W. Symes. Modeling of a constant q; methodology and algorithm for an efficient and optimally inexpensive viscoelastic technique. *Geophysics*, 60(1):176–184, February 1995.

Howard E. Boyer and Timothy L. Gall. *Metals Handbook: Desk*. Asm Intl, Metals Park, Ohio, desk edition edition, December 1984.

Roderic S. Lakes. *Viscoelastic Materials*. Cambridge University Press, April 2009.

Hsi-Ping Liu, Don L. Anderson, and Hiroo Kanamori. Velocity dispersion due to anelasticity; implications for seismology and mantle composition. *Geophysical Journal International*, 47(1):41–58, October 1976.

Claudio Madonna and Nicola Tisato. A new seismic wave attenuation module to experimentally measure low-frequency attenuation in extensional mode. *Geophysical Prospecting*, 61(2):302–314, 2013.

Edgar Manukyan, Hansruedi Maurer, Stefano Marelli, Stewart A. Greenhalgh, and Alan G. Green. Seismic monitoring of radioactive waste repositories. *GEOPHYSICS*, 77(6):EN73–EN83, November 2012.

Stefano Marelli, Edgar Manukyan, Hansruedi Maurer, Stewart A. Greenhalgh, and Alan G. Green. Appraisal of waveform repeatability for crosshole and hole-to-tunnel seismic monitoring of radioactive waste repositories. *Geophysics*, 75(5):Q21–Q34, September 2010.

R. J. O'Connell and B. Budiansky. Measures of dissipation in viscoelastic media. *Geophysical Research Letters*, 5(1):5–8, January 1978.

Nicola Tisato and Stefano Marelli. Laboratory measurements of the longitudinal and transverse wave velocities of compacted bentonite as a function of water content, temperature, and confining pressure. *Journal of Geophysical Research: Solid Earth*, 118(7):3380–3393, July 2013.

Nicola Tisato and Beatriz Quintal. Seismic attenuation in partially saturated rocks: recent advances and future directions. *The Leading Edge*, 33:640–646, 2014.